THERMAL OSCILLATION INDUCED BY AN INTERACTION BETWEEN SEA ICE AND OCEAN IN A NUMERICAL POLAR ICE-OCEAN MODEL

Satoshi SAKAI* and Shiro IMAWAKI**

* *Institute of Earth Science, Kyoto University, Sakyo-ku, Kyoto 606*
** *Geophysical Institute, Kyoto University, Sakyo-ku, Kyoto 606*

Abstract: A numerical model of simplified Arctic Ocean and Greenland-Norwegian Seas is presented. The essential effects of sea ice, river runoff, surface cooling, and water exchange between the Greenland-Norwegian Seas and the Atlantic Ocean are included. A thermal oscillation occurs due to an interaction between the sea ice and the ocean. The river runoff forms a low-salinity surface layer, which is essential to the oscillation. Parameters governing the time scale of the oscillation are also discussed.

1. Introduction

The world ocean circulation contributes to climatic control by means of the poleward heat transport. The oceanic heat transport is as large as the atmospheric transport in low and mid-latitudes (VONDER HARR and OORT, 1973; WUNSCH, 1980). The heating and cooling at the sea surface drive the thermohaline circulation of the world ocean, and the circulation transports the heat from low latitudes to high latitudes. The process of heat transfer through the sea surface is essentially important to determine the amount of the poleward transport. In the polar region, this process is complex because the sea surface is covered by the sea ice and the heat transfer from the ocean to the atmosphere is seriously reduced.

Although the effect of the sea ice on the atmosphere has been intensively studied (HERMAN and JOHNSON, 1978; WALSH and JOHNSON, 1979; PARKINSON and HERMAN, 1980), there have been few studies of the interaction between the sea ice and the ocean. SEMTNER (1976) simulates the current in the Arctic Ocean by a three-dimensional numerical model including the sea ice in a primitive way. His model, however, is not adequate to clarify the elementary physical features of the interaction between the sea ice and the ocean, because his model is complicated by many effects such as wind stress or intricate basin geometry together with river runoff and the supply of the Atlantic water.

In the present paper, the basin geometry is modeled as simple as possible. Only thermal and haline forcings are applied in order to study the elementary physics of an ice-covered ocean.

2. Model

The Arctic Ocean and the Greenland-Norwegian Seas are simply modeled as

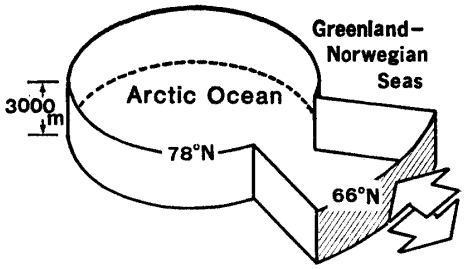

Fig. 1. Schematic figure of a model basin. The shaded portion is an open boundary, which borders on the Atlantic Ocean.

illustrated in Fig. 1. At an open boundary (66°N), an inflow and outflow are specified to represent a part of the thermohaline circulation in the Atlantic Ocean. The freshening effect due to the river runoff is included. Precipitation and evaporation at the sea surface are not considered, nor are bottom stress, wind stress, or side wall stress. The details of the model are as follows.

2.1. Open boundary

A zonal open boundary is designed to border on the Atlantic Ocean. Inflows are specified at the upper 3 levels and outflows at the lower 2 levels (Fig. 2). The velocity at each level is uniform horizontally. The transport of the inflow is 8×10^6 m^3/s. It is exactly equal to that of the outflow; the total volume transport across the open boundary vanishes. These inflows and outflows are a simplification of the observed water exchange between the Greenland-Norwegian Seas and the North Atlantic Ocean (WORTHINGTON, 1970).

The temperature and salinity of the inflow water are specified according to

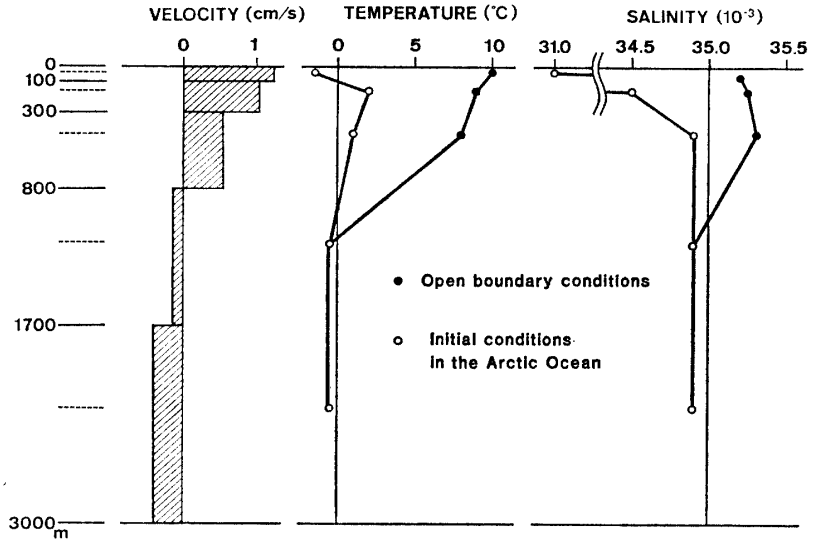

Fig. 2. Open boundary conditions of velocity, temperature and salinity, and initial conditions of temperature and salinity in the Arctic Ocean. Positive velocity indicates inflow. Temperature and salinity of the lower 2 levels at the open boundary are not fixed. The levels indicated in the left hand side of the figure are the levels assigned to the temperature, salinity, density, horizontal component of velocity (- - -) and the levels assigned to the vertical velocity (—).

oceanographic data observed south of Iceland (STEELE *et al.*, 1962). Slight horizontal variations are added so that the prescribed density field is geostrophically balanced with the specified velocity shear. The profiles in Fig. 2 are those at the center of the boundary. The temperature and salinity of the outflow water are made equal to the predicted values at the upstream grid points.

These open boundary conditions are appropriate if the Arctic Ocean and Greenland-Norwegian Seas do not alter the conditions of the Atlantic Ocean. This assumption is valid on a shorter time scale than the relaxation time of the Atlantic Ocean, which is, for example, estimated at 400 years for the density field by SERGIN (1979).

2.2. *Sea ice*

The sea ice primarily has two effects on the oceanic thermal balance: (1) It has a strong insulation effect on the heat transfer from the ocean to the atmosphere; (2) It considerably increases the albedo of the earth's surface, *i.e.* it considerably prevents the solar energy from penetrating into the ocean. These two effects oppositely act on the ocean; when the sea ice increases in area, effect (1) produces an oceanic heat gain and effect (2) produces an oceanic heat loss.

In the Arctic and subarctic seas, the net oceanic heat loss, including both effects, through the ice-free sea surface is some 75 kcal/(cm^2 year) (WORTHINGTON, 1970), whereas that through the ice-covered sea surface is typically 1–2 kcal/(cm^2 year) (MAYKUT and UNTERSTEINER, 1971). These observational estimates indicate that effect (1) exceeds effect (2) and the heat loss through the sea surface is positive regardless of the existence of the sea ice, although its amount is seriously reduced when the sea ice is present.

The sea ice is modeled according to SEMTNER (1976) in a following way.

(i) The sea ice forms if the sea surface temperature drops below -2°C.

(ii) The sea ice reduces the net heat flux by a factor of 40.

Exchange of latent heat associated with the ice formation is not considered. The net heat flux through the ice-free sea surface is taken to be 64 kcal/(cm^2 year) (SEMTNER, 1976) all over the basin.

2.3. *Fresh water*

Many rivers feed into the Arctic Ocean. The fresh water from these rivers forms a low-salinity layer just below the sea surface. This layer of low density tends to prevent thermal convection induced by the surface cooling. The volume of the river runoff is estimated at 85×10^3 m^3/s by COACHMAN and AAGAARD (1974). It is smaller by two orders of magnitude than the volume of the water exchange between the Greenland-Norwegian Seas and the Atlantic Ocean. The effect of the river runoff is included as a constant negative salt flux (without the mass flux) at the perimeter of the Arctic Ocean surface. The total salt flux is set as -2.2×10^{14} g/day, which corresponds to the above-mentioned volume of the river runoff if the salinity of the surface water is assumed to be 30×10^{-3}.

2.4. *Numerical scheme*

The numerical ocean model is almost the same as that of TAKANO (1974).

The density is computed from a polynomial formula by BRYAN and COX (1972). Convective adjustment is used when the predicted density field is gravitationally unstable. The stability is examined by comparison between the *in situ* water density at the upper level and the density that the lower level water would acquire if it were raised to that upper level.

An unusual spherical coordinate system is chosen to avoid coordinate singularity at the pole (SEMTNER, 1976); the equator of the coordinates passes through the North Pole. Grid size is about 220 km × 220 km horizontally and 5 levels are taken vertically.

The subgrid scale eddies are parameterized as eddy viscosity and diffusion in conventional parabolic formula. The coefficients of lateral viscosity and diffusion are taken to be 2×10^8 cm^2/s and 10^8 cm^2/s, respectively. The coefficients of vertical viscosity and diffusion are 1 cm^2/s.

Multiple time steps are used for the velocity field and the density field as in BRYAN *et al.* (1975). The time step for the velocity field is 1 day, and that for the density field is 2 days. This scheme of multiple time steps does not affect the solution when either the velocity field or the density field is in a steady state. In the present experiment, use of this scheme little affects the thermal variations because the velocity field scarcely changes after a set-up period. The time in the present paper refers to the time for the density field.

2.5. *Initial conditions*

The flow is initially confined only to the Greenland-Norwegian Seas. Meridional components of the velocities decrease linearly from 66°N to 78°N. Zonal components are taken to be zero. In the Arctic Ocean, the temperature and salinity are uniform horizontally in the initial state. Their vertical profiles are specified following COACHMAN and AAGAARD (1974) as indicated in Fig. 2. In the Greenland-Norwegian Seas, the temperature and salinity are determined by a linear interpolation of the values in the Arctic Ocean (78°N) and the values at the open boundary (66°N).

3. Thermal Oscillation

Numerical time integration is carried out for 240 years. Figure 3 shows the velocity fields at year 140. The velocity pattern scarcely changes after the set-up period of about 60 years. The velocities in the Arctic Ocean are very small compared with those in the Greenland-Norwegian Seas. In the present experiment, the horizontal advection has a minor role to determine the density field in the Arctic Ocean compared with the lateral diffusion of the temperature and salinity. Here, the discussions are confined to the density field.

A time series of the total heat contained in the whole basin is shown in Fig. 4a. It shows an apparent oscillation with a period of about 60 years. It does not seem to be a transient oscillation approaching a steady state, but a kind of self-excited oscillation. A time series of the total heat flux through the sea surface is shown in Fig. 4b. This value is nearly equal to the heat flux in the ice-free region. The

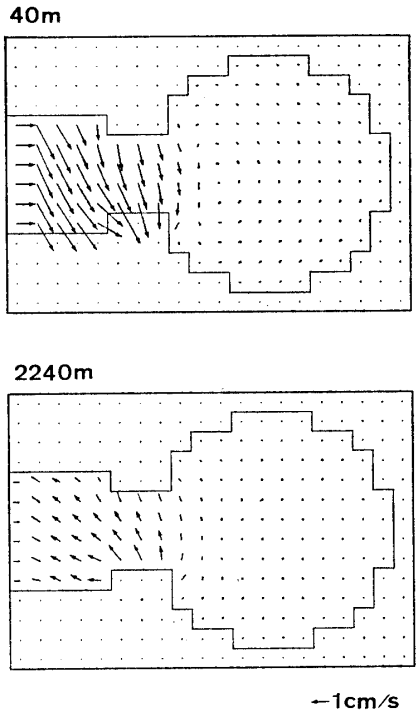

Fig. 3. Horizontal velocity fields at depths of 40 m and 2240 m in year 140. The lengths of the arrows are proportional to the velocity.

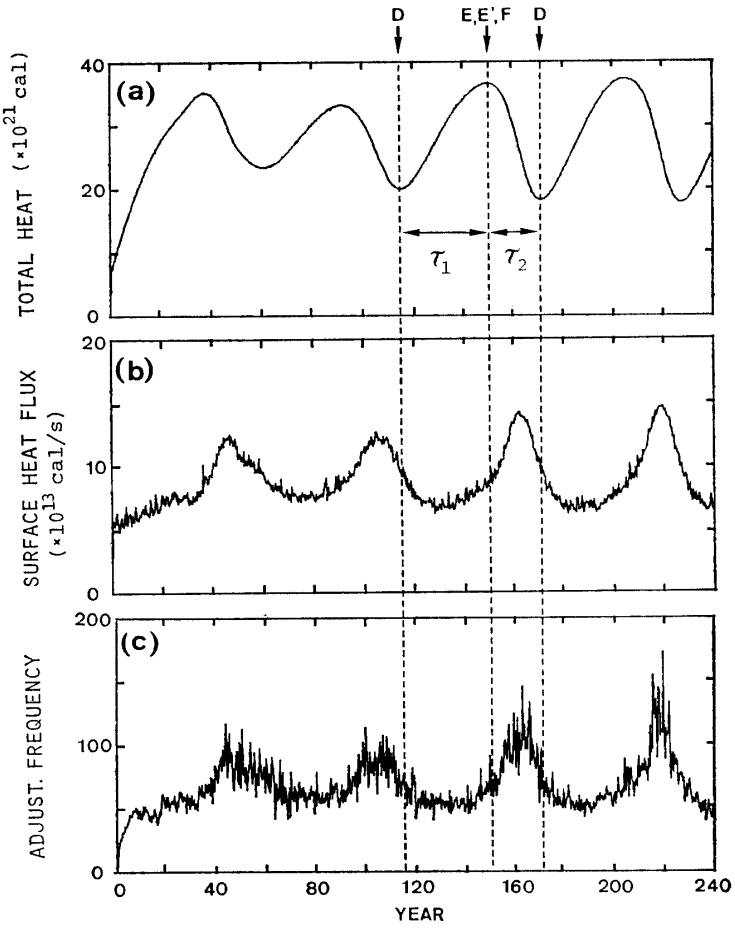

Fig. 4. Time histories of (a) the total heat contained in the whole basin, (b) the total surface heat flux from the ocean to the atmosphere, and (c) the frequency of the convective adjustment. The broken lines indicate the stages shown in Fig. 6.

oscillation of the total heat contained in the whole basin is caused mostly by the variation of this surface heat flux, because the heat flux through the open boundary is almost constant with time. The variation of the surface heat flux is highly correlated with the variation of the frequency of convective adjustment (Fig. 4c), which is calculated by summing up the repetition times of the convective adjustment at each point all over the basin. This frequency represents the frequency of occurrences of the gravitational instability.

Temperature and salinity fields at year 140 and year 160 are shown in Fig. 5. A thin layer of cold (0°C to −2°C), low-salinity (34.2×10^{-3} to 34.9×10^{-3}) water is clearly seen just below the ice-covered sea surface at year 140, but it has almost disappeared before year 160. The horizontal distributions of the frequency of the convective adjustment averaged over 12 successive time steps are shown in Fig. 5d. These two sets of figures show that the low-salinity layer disappears due to the gravitationally unstable density stratification in the Arctic Ocean.

The oscillation mechanism is summarized as follows. Three major external

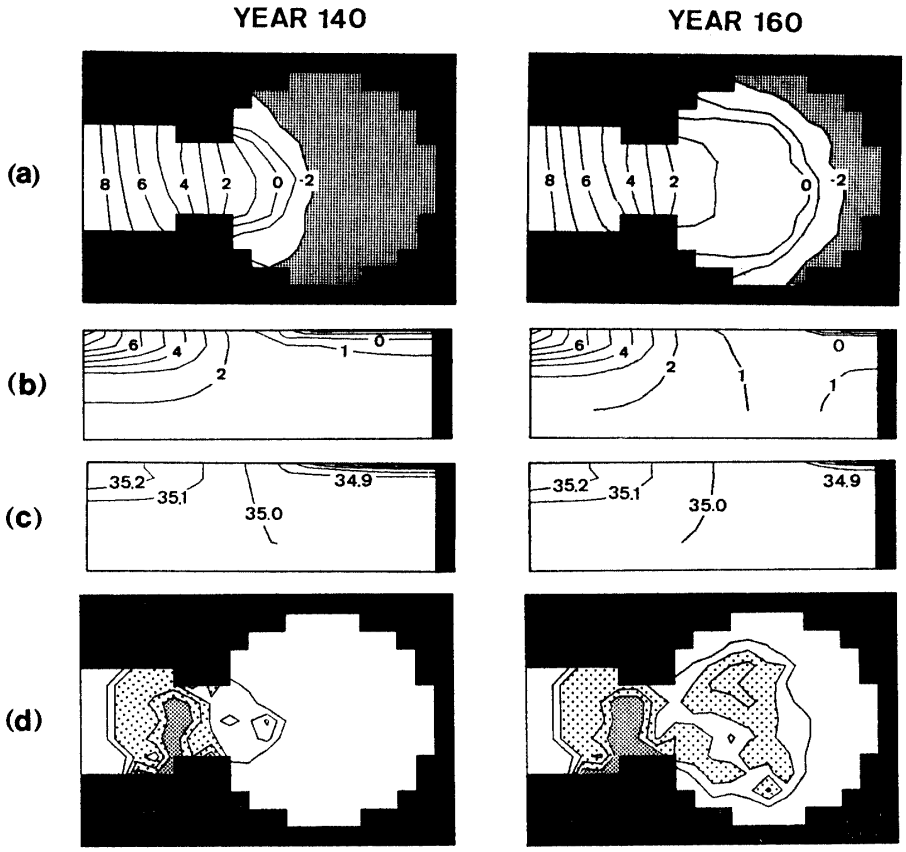

Fig. 5. (a) Horizontal distributions of the surface temperature in °C (shaded portion is the ice-covered region), (b) vertical distributions of the temperature (in °C) in a cross-section through the North Pole, (c) vertical distribution of the salinity (in 10^{-3}) in the same section as in (b), and (d) horizontal distributions of frequency of the convective adjustment (the darker shade indicates the greater frequency).

forcings are applied: (I) Inflow of the high-salinity, warm water; (II) Cooling through the ice-free sea surface; (III) Freshening by the river runoff. For the salinity budget, the negative salt flux imposed by forcing (III) almost balances with the positive salt flux through the open boundary by forcing (I). The model water can be classified into two types: a surface water and a deep water. A schematic temperature-salinity diagram (Fig. 6) helps in the understanding of the oscillation mechanism.

Suppose that the initial states of both surface and deep waters are represented by a point D at the freezing point. As time goes on, the temperature and salinity of the deep water rise at constant rates due to the relatively warm, high-salinity inflowing water [forcing (I)]. The deep water takes a path D–E in Fig. 6 and obtains buoyancy gradually with time.

On the other hand, the surface temperature is kept just below the freezing point, because the surface cooling is reduced by the sea ice as soon as the temperature of the surface water drops below the freezing point. The river runoff rapidly forms a thin low-salinity layer, which prevents a density instability due to a temperature inversion. Therefore, the surface water takes a path D–E′ under forcing (III) independent of the deep water.

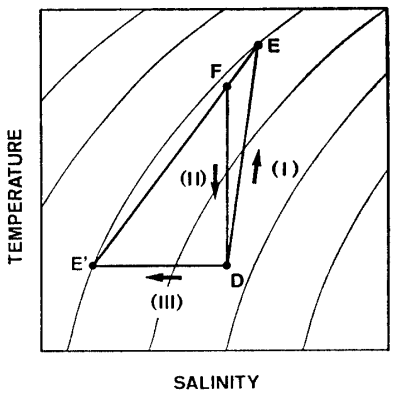

Fig. 6. Schematic temperature-salinity diagram of the surface and deep waters during a cycle of the thermal oscillation. Isopleths of density are also shown.

As the thickness of this low-salinity layer increases by vertical diffusion, the freshening rate for a unit mass decreases because the negative salt flux is constant with time. When the buoyancy of the deep water exceeds the buoyancy of the surface water, the two waters are mixed with each other by vertical overturning and the properties represented by a point F in Fig. 6 are obtained. In this state, the cold, low-salinity surface layer and the sea ice vanish. The density field is always unstable because of the strong surface cooling [forcing (II)]. The temperature of the entire water column drops until it reaches the freezing point D. Thereupon the surface and deep waters take independent ways again.

4. Time Scale of the Oscillation

The time scale of the present thermal oscillation is roughly estimated as follows. The mean area A_0 of the ice-free region is defined by

$$A_0 = Q_0/q\,, \tag{1}$$

where Q_0 is the net heat flux through the open boundary, q the surface heat flux through a unit area in the ice-free region. The areas of the ice-free regions A_1 in the process D–E and A_2 in the process F–D can be written as

$$A_1 = A_0 - \Delta A_1\,, \tag{2}$$

$$A_2 = A_0 + \Delta A_2\,, \tag{3}$$

where ΔA_1 and ΔA_2 are the deviations from the mean area A_0. If the heat flux through the sea ice is ignored, the heating rate in the process D–E can be written as $\Delta A_1 q$ and the cooling rate in the process F–D can be written as $\Delta A_2 q$. The heat capacity C_0 of the oscillating region is estimated by

$$C_0 = c(\Delta A_1 + \Delta A_2)H\,, \tag{4}$$

where c is the specific heat of the water, and H the water depth. Consequently the time scales τ_1 for the process D–E and τ_2 for the process F–D are

$$\tau_1 = c(1 + \Delta A_2/\Delta A_1)H\Delta T/q\,, \tag{5}$$

$$\tau_2 = c(1 + \Delta A_1/\Delta A_2)H\Delta T/q\,, \tag{6}$$

where ΔT is the temperature difference between D and E. Here, the relatively small heat capacity of the surface water is ignord. The period of the oscillation is $\tau_1 + \tau_2$ because the time scale for the process E–F or E′–F is negligible.

If the oscillation of the ice-covered area is symmetric about A_0, *i.e.* $\Delta A_1 = \Delta A_2$, the sum of eqs.(5) and (6) gives the minimum value and the period of the oscillation becomes 19 ΔT years for the parameters in the present model; $q = 64$ kcal/(cm^2 year) and $H = 3000$ m. The present experiment shows an asymmetric oscillation ($\Delta A_1/\Delta A_2 = 1/2$) with the temperature difference ΔT of 3°C, which results in an oscillation period of 63 years. This value closely agrees with the period observed in this experiment.

The temperature difference ΔT, at which the water column becomes unstable, is a function of the salinity stratification. If the salinity is vertically uniform, ΔT reduces to zero. This implies that no oscillation occurs. An experiment is carried out excluding the river runoff. The result shows no oscillation and the density field approaches a steady state.

5. Discussion

The present experiment shows that a self-excited thermal oscillation arises in the simplified Arctic Ocean model from the interaction between the sea ice and the ocean. To the authors' knowledge, however, such an oscillation has not yet been reported observationally. This is because in the real Arctic Ocean the density stratification by the salinity difference is too strong for the water column to overturn; the salinity difference between the surface and deep waters is typically $2\text{–}5 \times 10^{-3}$ in the real Arctic Ocean at the present age, whereas it is typically 0.5×10^{-3} in the present experiment. The thermal oscillation requires that the salinity difference between the surface and deep waters be less than 1.5×10^{-3}; otherwise the temperature inversion ΔT must be greater than 10°C. It is not well known why the salinity stratification in the present experiment is weak enough for the thermal oscillation to occur in spite of the realistic haline forcings. Although the thermal oscillation seems to be unrealistic at the present age, it might take place if the volume of the inflowing fresh water substantially decreases.

Some problems of the present model are noted below in comparison with the real Arctic Ocean. In the present model, the coefficient of the horizontal eddy diffusion is taken to be 10^8 cm^2/s and the horizontal heat transport is controlled mostly by the eddy diffusion in the Arctic Ocean. The coefficient seems to be relatively large. An experiment with a smaller coefficient of the eddy diffusion might give results different from the present ones.

Vertical overturning induced by the gravitationally unstable stratification is parameterized by the simple convective adjustment technique. The sea ice is modeled also in a simple way. Their essential effects are included in the present model, but further studies are required because they are very important in the polar ocean.

The bottom topographic features in the Arctic Ocean are neglected. The most important feature is probably the continental shelf off the Siberian coast, where a great deal of high-salinity shelf water is formed. The volume of the shelf water is estimated to be as much as the volume of the water exchange between the Atlantic Ocean and the Greenland-Norwegian Seas (AAGAARD *et al.*, 1981). This

process is thought to have a significant effect on the haline circulation.

Although wind stress is not included, it can induce a horizontal circulation, which might alter the density field in the Arctic Ocean.

The present experiment indicates that the Arctic Ocean has a potential thermal oscillation with a period of several tens of years, but the probability of the oscillation actually occurring should be carefully examined by further studies concerning all problems noted above.

Acknowledgments

The authors wish to thank Prof. H. KUNISHI of Kyoto University for his guidance and encouragement. Prof. K. Takano of the University of Tsukuba is also acknowledged; he readily allowed us to use his program of a numerical ocean model. The numerical computations were carried out on the FACOM M-200 at the Data Processing Center, Kyoto University. This work was done under the Polar Experiment (POLEX) program.

References

AAGAARD, K., COACHMAN, L. K. and CARMACK, E. (1981): On the halocline of the Arctic Ocean. Deep-Sea Res., **28**, 529–545.

BRYAN, K. and COX, M. D. (1972): An approximate equation of state for numerical models of ocean circulation. J. Phys. Oceanogr., **2**, 510–514.

BRYAN, K., MANABE, S. and PACANOWSKI, R. C. (1975): A global ocean-atmosphere climate model. Part II. The oceanic circulation. J. Phys. Oceanogr., **5**, 30–46.

COACHMAN, L. K. and AAGAARD, K. (1974): Physical oceanography of Arctic and subarctic seas. Marine Geology and Oceanography of the Arctic Seas, ed. by V. HERMAN. New York, Springer-Verlag, 1–72.

HERMAN, G. F. and JOHNSON, W. T. (1978): The sensitivity of the general circulation to Arctic sea ice boundaries: A numerical experiment. Mon. Weather Rev., **106**, 1649–1664.

MAYKUT, G. A. and UNTERSTEINER, N. (1971): Some results from a time-dependent thermodynamic model of sea ice. J. Geophys. Res., **76**, 1550–1575.

PARKINSON, C. L. and HERMAN, G. F. (1980): Sea ice simulations based on field generated by the GLAS GCM. Mon. Weather Rev., **108**, 2080–2091.

SEMTNER, A. J. (1976): Numerical simulation of the Arctic Ocean circulation. J. Phys. Oceanogr., **6**, 409–425.

SERGIN, V. Y. (1979): Numerical modeling of the glaciers-ocean-atmosphere global system. J. Geophys. Res., **84**, 3191–3204.

STEELE, J. H., BARRETT, J. R. and WORTHINGTON, L. V. (1962): Deep currents south of Iceland. Deep-Sea Res., **9**, 465–474.

TAKANO, K. (1974): A general circulation model for the world ocean. Numerical Simulation of Weather and Climate, Tech. Rep., No. 8, Los Angeles, University of California, 46 p.

VONDER HARR, T. H. and OORT, A. H. (1973): New estimate of annual poleward energy flux by northern hemisphere oceans. J. Phys. Oceanogr., **3**, 169–172.

WALSH, J. E. and JOHNSON, C. M. (1979): Interannual atmospheric variability and associated fluctuations in Arctic sea ice extent. J. Geophys. Res., **84**, 6915–6928.

WORTHINGTON, L. V. (1970): The Norwegian Sea as a mediterranean basin. Deep-Sea Res., **17**, 77–84.

WUNSCH, C. (1980): Meridional heat transport of the North Atlantic Ocean. Proc. Natl. Acad. Sci. USA, **77**, 5043–5047.

(Received May 11, 1982; Revised manuscript received July 31, 1982)